Molecular Cancer Therapeutics

AC0010, an Irreversible EGFR Inhibitor Selectively Targeting Mutated EGFR and Overcoming T790M-Induced Resistance in Animal Models and Lung Cancer Patients

Xiao Xu[1,2], Long Mao[1,2], Wanhong Xu[1], Wei Tang[1], Xiaoying Zhang[1], Biao Xi[2], Rongda Xu[1,2], Xin Fang[1], Jia Liu[1,2], Ce Fang[2], Li Zhao[2], Xiaobo Wang[1,2], Ji Jiang[3], Pei Hu[3], Hongyun Zhao[4], and Li Zhang[4]

Abstract

AC0010 is a pyrrolopyrimidine-based irreversible EGFR inhibitor, structurally distinct from previously reported pyrimidine-based irreversible EGFR inhibitors, such as osimertinib and rociletinib. AC0010 selectively inhibits EGFR-active and T790M mutations with up to 298-fold increase in potency compared with wild-type EGFR. In a xenograft model, oral administration of AC0010 at a daily dose of 500 mg/kg resulted in complete remission of tumors with EGFR-active and T790M mutations for over 143 days with no weight loss. Three major metabolites of AC0010 were tested and showed no wild-type EGFR inhibition or off-target effects, such as inhibition of IGF-1R. AC0010 is safe in non–small cell lung cancer (NSCLC) patients at a dose range between 50 and 550 mg once per day, and no hyperglycemia or other severe adverse effects were detected, such as grade 3 QT prolongation. The objective responses were observed in NSCLC patients with EGFR T790M mutation. *Mol Cancer Ther; 15(11); 2586–97. ©2016 AACR.*

Introduction

Non–small cell lung cancer (NSCLC) accounts for approximately 85% of all lung cancers and is often insidious, and around 80% of patients have more advanced disease, including 25% of patients with regional metastasis and 55% of patients with distant spread of disease (1, 2). In the previous decade, a more comprehensive molecular understanding of the pathology of NSCLC has led to the development of small molecules that target genetic mutations known to play critical roles in the progression to the metastatic disease in NSCLC patients, such as mutations in EGFR and ALK (3–5). EGFR is expressed on the cell surface of a substantial percentage of NSCLCs, and 15% to 40% of total NSCLC patients harbor mutations in EGFR. Studies with the EGFR tyrosine kinase inhibitors (TKI), gefitinib and erlotinib, demonstrated biological and clinical activity in a subset of lung cancers harboring EGFR-active mutations, such as small deletions (delE747–750) and point mutation at codon 858 (L858R; refs. 6–9). Despite the impressive results of genotype-directed therapy, EGFR-active mutation-positive patients eventually develop resistance (10, 11). There are at least two mechanisms that contribute to the acquired resistance: (i) the emergence of the gatekeeper T790M EGFR mutation, which prevents binding of the gefitinib and erlotinib to EGFR; and (ii) the upregulation of a bypass track that activates downstream signals (12–15). As reported, more than 50% of patients who developed resistance have the T790M mutation (16). An experimental compound, WZ4002, and two clinical compounds, osimertinib and rociletinib, reported as third-generation EGFR TKIs, demonstrated the inhibition of EGFR T790M-resistant mutation in animal models and in patients (17–19).

AC0010 was designed specifically to inhibit EGFR-active mutations and the T790M-acquired resistant mutation, while sparing wild-type EGFR. In the preclinical studies, AC0010 showed potent inhibition of NSCLC that harbors both active mutation(s) and T790M mutation in three xenograft mouse models. In addition, AC0010 and its metabolites result in no observable off-target side effects, such as hyperglycemia and grade 3 QT prolongation, and appear to contain a safe profile in animal models and in patients. Importantly, AC0010 overcame T790M-induced resistance to first-generation EGFR drugs in NSCLC patients. It is therefore warranted to further develop AC0010 as an alternative therapeutic agent for NSCLC patients who develop acquired resistance to first-generation EGFR TKIs.

Materials and Methods

Structural chemistry

Experimental drugs or chemicals, gefitinib, afatinib, and AZ5104 were purchased from Jinan XuanHong Pharmaceutical

[1]ACEA Pharmaceutical Research, Hangzhou, Zhejiang, P.R. China. [2]ACEA Biosciences Inc., San Diego, California. [3]Peking Union Medical College Hospital, Beijing, P.R. China. [4]Cancer Center, Sun Yat-Sen University, Guangzhou, Guangdong, P.R. China.

Note: Supplementary data for this article are available at Molecular Cancer Therapeutics Online (http://mct.aacrjournals.org/).

Corresponding Authors: Xiao Xu, ACEA Biosciences Inc., 6997 Mesa Ridge Road, Suite 100, San Diego, CA 92121. Phone: 858-724-0928; Fax: 858-724-0927; E-mail: xxu@aceabio.com; and Li Zhang, Cancer Center, Sun Yat-Sen University, Guangzhou, Guangdong, P.R. China. Phone: 020-8734-2288; Fax: 020-8734-2288; E-mail: zhangli6@mail.sysu.edu.cn

doi: 10.1158/1535-7163.MCT-16-0281

Technology Co., Ltd., China Langchem Inc., and Selleckchem, respectively. AC0010 (freebase), AC0010MA (maleate salt), AC0010 metabolites MII-2, MII-6, and M7, rociletinib, and osimertinib were synthesized by Hangzhou ACEA Pharmaceutical Research Co., Ltd.

Molecular modeling/docking structures were conducted using Schrodinger LigPrep, Glide and Maestro programs. The crystal structure of T790M-mutant EGFR in complex with WZ4002, HKI-272, and AEE788 was retrieved from the protein data bank (PDB entry 3IKA, 2JIV, and 2JIU, respectively). Water cluster analysis was performed by running scripts from Schrodinger software. Docking was performed with the Glide program (Schrodinger). The Protein Preparation Wizard module of Maestro was used to prepare the protein. During protein preparation, all water molecules were deleted, except the 4 conserved water molecules within 10 Å distance of WZ4002. For docking, the scoring grids were centered on the crystal structure of WZ4002 using the default bounding box sizes, with an inner box of 10 Å on each side and an outer box of 24 Å on each side. Flexible docking with default parameters was used. Glide XP (extra precision) was employed for all docking calculations. The best docked poses were selected as the ones with the lowest GlideScore.

Cell culture

The NCI-H1975, HCC827, A431, A549, NCI-H460, HT1080, HeLa, BEAS-2B, and NIH/3T3 cells were obtained from ATCC in the years 2011 to 2013 and maintained at 37°C with 5% CO_2 in the media supplemented with 10% FBS (HyClone), penicillin (100 U/mL), and streptomycin (100 μg/mL). All cell lines were authenticated at ATCC using short tandem repeat profiling and cultured for fewer than 3 months after resuscitation. Cells were routinely screened for mycoplasma and periodically authenticated by morphologic inspections.

Engineered cell lines and resistant cell lines

NIH/3T3 cells harboring EGFR L858R/T790M double mutations were engineered by exposing NIH/3T3 cells to the lentivirus that expressed human EGFR (L858R/T790M), and then followed by clone selection using puromycin. The resistant colonies were selected and expanded for further sequencing analysis to confirm the integration of EGFR L858R/T790M mutations. A confirmed clone was subsequently established to be a cell line designated as NIH/3T3_TC32T8.

Resistant cell line NCI-H1975-P1 was derived from relapsed tumor tissues of NCI-H1975 xenograft mouse that developed resistance to AC0010. AC0010-resistant NCI-H1975-AVR1 cells and osimertinib-resistant NCI-H1975-OSR1 cells were generated *in vitro* by exposing NCI-1975 cells to escalating doses of AC0010 and osimertinib, respectively, for a prolonged period.

Cell proliferation assays

Cell proliferation was assayed by a cell viability reagent, WST-1, per instruction from the manufacturer (Roche). Cells were seeded at optimal density onto 96-well plates and incubated for 24 hours, followed by compound treatment for 72 hours. Cell viability was then assayed by incubating cells with WST-1 reagent for 2 to 3 hours.

Immunoblotting analysis

NCI-H1975, HCC827, and A431 cells were seeded onto 6-well plates at a density of 1×10^6 cells per well. After 24 hours of culture, cells were then incubated in serum-free media for 1 hour and treated with test compound for 2 hours. A431 cells were stimulated with 30 ng/mL EGF during the last 15 minutes of compound treatment. Immunoblotting analysis was performed using whole-cell extracts, and the blots were probed with phospho-specific EGFR (p-Y1068), total EGFR, phospho-Akt (Ser-473), total Akt, phospho-ERK1/2 (p-T202/p-Y204), and total ERK1/2 antibodies (Cell Signaling Technology).

Immunoblotting analysis was performed with the tumor tissues isolated from mouse xenograft models to detect EGFR phosphorylation *in vivo*. The tumor tissues were homogenized in RIPA buffer supplemented with protease inhibitors and phosphatase inhibitors, and the homogenized solutions were incubated on ice for 30 minutes, followed by two rounds of centrifugation at 14,000 rpm for 30 minutes at 4°C. The supernatants were collected for immunoblotting analysis to probe p-EGFR, total EGFR, and β-tubulin as the protein-loading control. The densities of blotting bands were acquired and analyzed by ImageJ Software.

ELISA assay

Cells were seeded onto a 96-well plate, grown for 24 hours, and then treated with test compound in serum-free medium for 2 hours. NIH/3T3_TC32T8 and A431 cells were stimulated with 30 ng/mL EGF during the last 15 minutes of compound treatment. Cells were washed with ice-cold PBS before extraction with 100 μL cell lysis buffer. Phosphorylation of EGFR was measured using a sandwich ELISA assay with the pair of phospho-specific EGFR (pY1068) and total EGFR antibodies.

Xenograft models

All studies involving animal handling, care, and treatment were conducted in Hangzhou ACEA Pharmaceutical Research Co., Ltd. and performed according to the guidelines and SOPs approved by Department of Science and Technology of Zhejiang Province, China.

The Nu/Nu nude mice were purchased from Beijing Vital River Laboratories. Six- to 8-week-old female mice were inoculated subcutaneously at the right flank with approximately $3–5 \times 10^6$ cells in 0.2 mL of medium for tumor development. The treatments were started when the tumor size reached approximately 200 mm^3. For NCI-H1975 and A431 models, mice were divided into five groups ($n = 8$/group), including a vehicle group (0.5% methylcellulose), three AC0010-testing groups treated with AC0010MA at the doses of 12.5, 50, and 500 mg/kg, and a control group treated with gefitinib at 100 mg/kg. All mice were orally administrated once daily for 14 consecutive days.

For the long-term treatment study, NCI-H1975 tumor-bearing mice with tumor volume of 170 mm^3 were orally treated with a vehicle control (0.5% methylcellulose), AC0010 at dose levels of 12.5 and 50 mg/kg for 17 days when the tumor volume in vehicle control group reached approximately 2,000 mm^3. After 17-day dosing, animals in the vehicle control group were sacrificed, whereas animals in AC0010 groups were continually daily administrated with increased dose at 500 mg/kg till the test mice could not tolerate the treatment. Mouse body weight and tumor volume were measured twice per week. Tumor

volume was then used for the calculation of tumor inhibitory rate and tumor regression rate.

Pharmacokinetics, pharmacodynamics, metabolites, and safety in animal models

Pharmacokinetics/pharmacodynamics. NCI-H1975 tumor-bearing mice with tumor volume of approximately 200 to 500 mm^3 were used in the pharmacokinetics/pharmacodynamics study. The dose levels of AC0010 for oral administration were 12.5, 50, and 200 mg/kg with either single administration or 8 consecutive day treatments, while intravenous dose was singly administered at 10 mg/kg. Vehicle control (0.5% methylcellulose) and gefitinib at 100 mg/kg were also orally administered for 1 day or 8 consecutive days. Blood samples were collected predose and at 0.0833, 0.25, 0.50, 1, 2, 4, 6, 8, and 24 hours postdose, and tumor tissues were collected predose and at 1, 4, 8, and 24 hours postdose. Tumor tissues for 200 mg/kg AC0010 with 8-dose groups were not collected due to very small size of tumors that resulted from the treatments. The tumor tissues were cut into two parts for assaying L858R/T790M EGFR phosphorylation by immunoblotting analysis and for measuring AC0010 concentrations in the tumor tissues. The densities of blotting bands analyzed by ImageJ software were used for deriving pEGFR/EGFR values. The AC0010 concentrations in plasma and tissues were analyzed by the LC/MS-MS methods.

Metabolite analysis. Metabolite profiling was conducted for AC0010 *in vitro* in mouse, rat, dog, monkey, and human liver microsomes as well as *in vivo* in rat plasma, feces, and urine samples. All samples were analyzed by an LC/MS-MS system. The structures of major metabolites were elucidated on the basis of EPI spectra and further confirmed by using synthesized authentic standards. Selected metabolites were quantified in multiple reaction monitoring mode in rat and monkey GLP toxicokinetic study samples as well as in human clinical samples. The biological activities of AC0010 and its metabolites against wild-type and mutant EGFR were assessed using WST cell proliferation assay and p-EGFR ELISA assay. The general toxicity was assayed against a panel of A549, HT1080, HeLa, NCI-H460, and Beas-2B cells.

Clinical studies

Study design. This was a single-center, open-label, two-stage, single/multiple doses, and dose–escalation phase I study in histologically confirmed metastatic or unresectable locally advanced NSCLC patients. The main inclusion/exclusion criteria were described in the protocol (NCT 02274337). The criteria of acquired resistance to EGFR TKIs, for example, gefitinib and erlotinib, were used on the basis of the clinical definition by Jackman and colleagues (10).

On the basis of the modified Fibonacci methods, five dose cohorts were designed, including 50 mg/d, 100 mg/d, 200 mg/d, 350 mg/d, and 550 mg/d. Dose-limiting toxicity (DLT) was defined as an adverse event (AE) occurring during cycle one following the Common Terminology Criteria for Adverse Events Version 4.0 (CTCAE v4.0) criteria. All patients were treated with AC0010 on trial NCT 02274337, with written informed consent from patients and approval by Sun Yat-Sen University Cancer Center Ethics Committee. The permission for publishing patients' image scan results is included in the informed consent.

Patients' treatment and pharmacokinetic analysis. The clinical pharmacokinetic study of AC0010 was performed for both single dose and multiple doses. Blood samples were collected from each subject at prespecified times after the single dose (predose, 1, 2, 3, 4, 5, 6, 8, 12, 24, and 48 hours postdose) and during the multiple dosing cycles (cycle 1 at pre-ose on days 1, 8, 15, and 22, as well as at predose, 0.5, 1, 2, 3, 4, 6, 8, 12, and 24 hours postdose on day 28).

Results

AC0010 as a novel covalent EGFR TKI demonstrates an inhibitory activity selectively against the mutant EFGR *in vitro*

Using structure-based drug design and focused compound library screening approach, a novel series of irreversible small-molecule inhibitors was selected. Many of them showed specific inhibition with different extent of potency to EGFR-active mutations, such as L858R, delE746–750, and T790M. Furthermore, these series of compounds displayed enhanced selectivity for the EGFR-active mutations over the wild-type EGFR (data not shown). Medicinal chemistry efforts, structure–activity relationship study, and structural optimization led to the discovery of the candidate compound, AC0010 (Fig. 1A), which showed the highest inhibitory potency against EGFR T790M mutation and the best selectivity over wild-type EGFR in the series (data not shown). AC0010 covalently modified recombinant EGFR T790M mutation at the target cysteine 797 amino acid (Supplementary Fig. S1). In comparison with the structures of other reported third-generation tyrosine kinase EGFR inhibitors (WZ4002, rociletinib, and osimertinib), the designed drug molecule AC0010 has a distinct chemical structure containing pyrrolopyrimidine ring system as its core (Fig. 1A), whereas all the other third-generation EGFR inhibitors, such as WZ4002, rociletinib, and osimertinib, have the pyrimidine core structure (17, 20–21). X-ray structure of EGFR T790M covalently bound to WZ4002 (left, PDB entry 3IKA), and docked structure of WZ4002 (middle) and AC0010 (right) are shown in Fig. 1B, using Schrödinger Maestro programs. The acrylamide groups on both WZ4002 and AC0010 are at a position that molecular modeling predicts to react with Cys797 (Fig. 1B, middle and right) and form H-bonds to Met793 backbone amide and carbonyl. In addition, the hydrogen from NH group of the pyrrole ring from AC0010 forms additional H-bond with Glu 791 backbone carbonyl oxygen. AC0010 ranks significantly higher than WZ4002 in docking analysis (docking scores of −9.640 and −6.812 for AC0010 and WZ4002, respectively), which may be related to the higher inhibitory effect of AC0010 on EGFR T790M mutations than other prymindine-based compounds, such as WZ4002, rociletinib, and osimertinib (Fig. 2A). In our assay system, the IC_{50} value of osimertinib on EGFR phosphorylation in NCI-H1975 was 214 ± 40 nmol/L. However, in the literature, the *in vitro* IC_{50} value of osimertinib was reported to be at 15 nmol/L (21). Here, the parallel experimental results were used.

In the kinase enzymatic assay, AC0010 exhibited potent inhibitory activity, with IC_{50} value of 0.18 nmol/L against EGFR L858R/T790M double mutations, nearly 43-fold greater potency over wild-type EGFR (IC_{50} value, 7.68 nmol/L; Supplementary Table S1). The inhibitory activity and selectivity of AC0010 were further evaluated in the NCI-H1975 and NIH/3T3_TC32T8 lines harboring EGFR L858R/T790M double mutations, the HCC827 line harboring delE746-A750

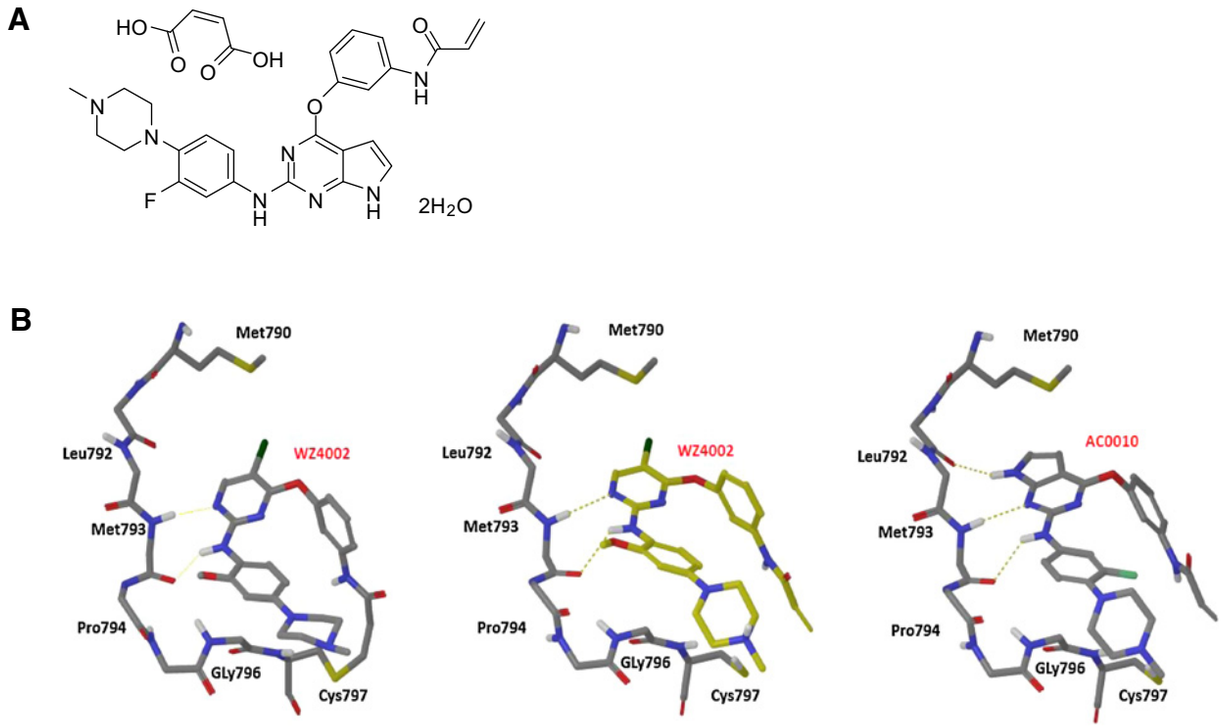

Figure 1.

AC0010 chemical structure and T790M EGFR-binding modes. **A,** chemical structure of AC010 maleate salt with dihydrate, which contains a pyrrolopyrimidine core. **B,** binding modes of WZ4002 and AC0010 in T790M EGFR ATP-binding site. Left, X-ray crystal structure of WZ4002 covalently bound to T790M EGFR (PDB: 3IKA); middle, docking structure of WZ4002 to T790M EGFR; right, docking structure of AC0010 to T790M EGFR. Schrödinger Maestro program was used for structure preparation and docking (see Materials and Methods for details).

mutation, and the A431 cell line, which expresses wild-type endogenous EGFR receptor. AC0010 selectively inhibited mutant EGFR phosphorylation with IC_{50} values of 7.3 and 2.8 nmol/L in NCI-H1975 and NIH/3T3_TC32T8 cells, about 115- and 298-fold more sensitive than that of the inhibition of wild-type EGFR in A431 (Fig. 2A). Consistent with the inhibitory effects of AC0010 on EGFR phosphorylation by ELISA assays, immunoblotting analysis confirmed that AC0010 potently inhibited EGFR-Tyr1068 phosphorylation in NCI-H1975 cells, and the selectivity ratio is at 65-fold for NCI-H1975 cells versus A431 cells (Fig. 2B). As expected gefitinib potently inhibited EGFR phosphorylation in the wild-type EGFR cells but not in the EGFR T790M mutation–harboring cells (Fig. 2C). In addition to inhibition of EGFR-Tyr1068 phosphorylation, AC0010 inhibited phosphorylation of the downstream targets Akt and ERK1/2, two important kinases involved in cancer cell proliferation and survival, in NCI-H1975 and HCC827 cells (Fig. 2B). Consistent with the EGFR phosphorylation data, AC0010 was much less potent at inhibiting Akt and ERK1/2 phosphorylation in wild-type EGFR cells. This is well correlated with the weak potency of AC0010 against wild-type EGFR (Y1068) phosphorylation with the IC_{50} value of 288 nmol/L in A431 cells. Collectively, the results from EGFR phosphorylation assays demonstrate that AC0010 is a novel third-generation EGFR TKI that inhibits EGFR T790M and other sensitive mutations but spares wild-type EGFR.

The selectivity of AC0010 was also assessed by testing its activity against a panel of 349 kinases. At a concentration of 1 μmol/L, AC0010 exhibited greater than 80% inhibition in 33 of 349 unique kinase assays (9.5%; Supplementary Fig. S2). Kinase targets with greater than 80% inhibition include JAK3, BTK, and 5 TEC family members (Supplementary Fig. S2). However, at the cellular level, the kinase-inhibitory potency is much less than with the enzymatic assay. For example, much weaker inhibition was seen in BTK and JAK3 cellular assays, with IC_{50} values of 59 and 360 nmol/L (Supplementary Table S1), demonstrating a favorable selectivity profile of AC0010.

To further evaluate the potential off-target liability of AC0010, it was tested against a selected panel of 55 key molecular targets, including receptors, ion channels, and transporters (Eurofins Express Profile; Supplementary Table S2). Of the 55 targets tested in the binding assay, five showed more than 50% inhibition of radioligand binding in the presence of 1 μmol/L AC0010, including adenosine A3, L-type calcium (Cav1.2) channel, dopamine transporter, 5-HT2A, and 5-HT2B (Supplementary Table S3). Cell-based functional assays were carried out to further characterize AC0010 interaction with the above five targets, and no inhibition was detected at the cellular level, implying that at pharmacologically relevant concentrations, the risk of off-target binding of AC0010 is minimal (Supplementary Table S3).

AC0010 inhibits EGFR-mutant tumor growth but not wild-type EGFR tumor growth in xenograft models over extended duration

Four types of xenograft mouse models, including NCI-H1975, HCC827, NIH/3T3_TC32T8, and A431 were used. Repeat daily

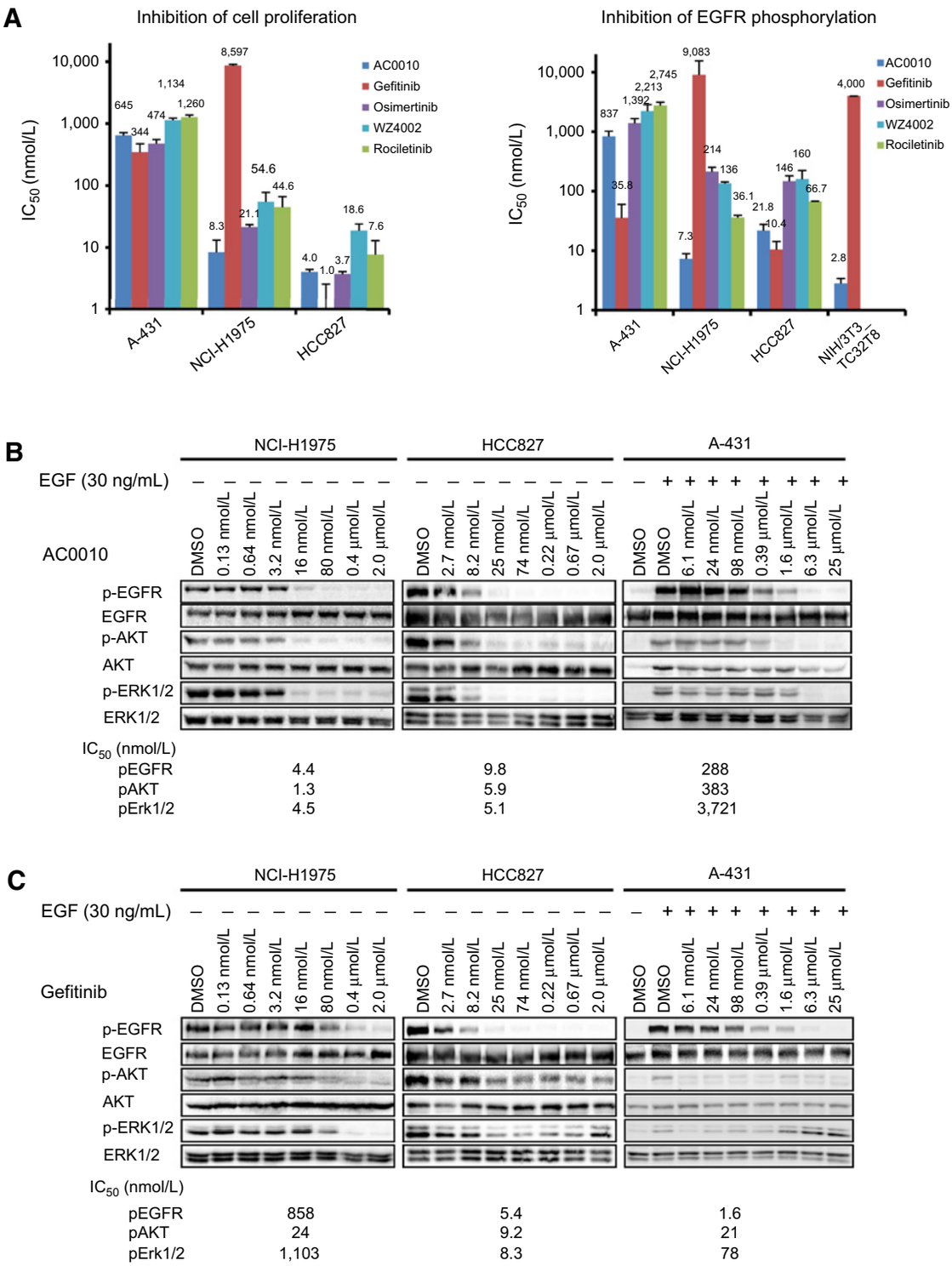

Figure 2.

Inhibition of cell proliferation and EGFR phosphorylation. **A,** comparison of the inhibitory activity of AC0010 to gefitinib and other third-generation EGFR TKIs on proliferation using WST assay and EGFR phosphorylation in NCI-H1975, HCC827, A431, and NIH/3T3_TC32T8 cells using ELISA. IC_{50} values shown on log10 scale in nmol/L as an average of three independent experiments ± SEM. **B,** AC0010 inhibition of phosphorylation of EGFR-Tyr1068 and its downstream signaling proteins Akt and ERK in NCI-H1975 cells, HCC827 cells, and wild-type EGFR cell line A431 using Western blot analysis. **C,** gefitinib inhibition of phosphorylation of EGFR-Tyr1068 and its downstream signaling proteins Akt and ERK in NCI-H1975 cells, HCC827 cells, and wild-type EGFR cell line A431 using Western blot analysis. IC_{50} values are derived from the density of blotting band of the whole-cell extracts after 2 hours of compound treatment.

oral administration of AC0010 at a dose range between 12.5 and 200 mg/kg resulted in a dose-dependent growth inhibition of all three tumors with EGFR-active mutations and T790M mutation but not with the wild-type EGFR (A431 model; Fig. 3A and B and Supplementary Fig. S3). At the dose level of 200 mg/kg, tumor regression was observed with the regression rates of 78%, 98%, and 25% in NCI-H1975, HCC827, and NIH/3T3_TC32T8 models, respectively. In contrast, gefitinib, at a dose of 100 mg/kg, showed no tumor growth inhibition in the NCI-H1975 and NIH/3T3_TC32T8 models harboring T790M. AC0010, at a dose of 200 mg/kg, did not exhibit any antitumor activity in the A431 xenograft model. As predicted, gefitinib showed strong inhibition in A431 xenograft model at the dose of 100 mg/kg (Fig. 3B).

To explore the pharmacokinetics/pharmacodynamics relationship *in vivo*, the plasma and tumor tissues from the AC0010-treated NCI-H1975 xenograft models were examined. For pharmacokinetic analysis, following intravenous administration of 10 mg/kg of AC0010, total body clearance and volume of distribution of AC0010 were estimated to be 5.91 L/h/kg and 14.76 L/kg, respectively. The elimination half-life ($t_{1/2}$) of AC0010 was about 1.73 hours, indicating AC0010 is rapidly distributed into tissues, including tumor tissues. Following oral administration of 12.5, 50, and 200 mg/kg of AC0010 for 1 day or 8 consecutive days, AC0010 was absorbed with the T_{max} of 1 to 2 hours, and bioavailability of 15.9% to 41.4%. AUC_{0-t} values of AC0010 from plasma were 333, 2,623, and 6,774 ng·h/mL on day 1, respectively, and 678, 3,476, and 7,299 ng·h/mL on day 8, respectively (Fig. 3C and D). To further study the pharmacodynamics of AC0010, the phosphorylation of mutant EGFR in tumor tissues was examined, showing complete inhibition by AC0010 after 4-hour treatment at the dose of 12.5 mg/kg, and the inhibition was sustained up to 8 hours (Fig. 3E). At the dose of 50 mg/kg, complete inhibition was achieved after 1-hour treatment, and such inhibition was sustained up to 8 hours. At the dose of 200 mg/kg, complete inhibition of phosphorylation was observed in tumor tissues through the measurement period from 1 to 24 hours. The dose-dependent inhibition of mutant EGFR phosphorylation in tumor tissues were well correlated with the *in vivo* efficacy and plasma and tissue concentrations of AC0010 in a parallel study (Fig. 3A, C, and D). Again, no inhibition of EGFR L858R/T790M phosphorylation was detected in the tumor sample treated with 100 mg/kg gefitinib (Fig. 3E).

Next, the duration of AC0010-induced tumor shrinkage in NCI-H1975 xenograft models was studied (Fig. 3F). In comparison with the vehicle control mice, the tumor growth inhibition rates were 71% and 79% in 12.5 and 50 mg/kg of dose groups, respectively, after 17 days dosing. To achieve the maximum efficacy and evaluate tolerability of AC0010 in long-term treatment, we selected the dose of 500 mg/kg and continued the daily dosing for another consecutive 143 days in the mice previously treated at 12.5 and 50 mg/kg. Significant tumor regression was quickly observed in all animals (total 14 mice) after first three doses of AC0010 at 500 mg/kg (day 21). The tumor volume became immeasurable from the starting value of 510 mm^3, indicating a very strong dose-dependent activity against EGFR T790M mutation–bearing tumors. During the dosing period of 143 days, 50% of mice showed complete remission of the tumors. Interestingly, tumor relapses were observed in 2 of 14 mice (14%). The relapses were found on day 106 and day 135 post AC0010 dosing and may indicate development of resistance against the AC0010 in NCI-H1975 tumor xenograft model. The mouse with the relapse on day 106 was sacrificed at day 115 when the tumor volume reached 660 mm^3 from the undetectable tumor. The relapsed tumor tissue was collected and an *in vivo* resistance cell line, NCI-H1975-P1, was generated. To test the cross-resistance of AC0010 with other third-generation EGFR TKIs, NCI-H1975-P1 together with NCI-H1975-AVR1 and NCI-H1975-OSR1, two resistant cell lines induced *in vitro* by AC0010 and osimertinib, were further investigated. The cross-resistance was seen between AC0010 and the other two third-generation compounds, rociletinib and osimertinib, in these three cell lines (Supplementary Table S4). Interestingly, in NCI-H1975-AVR1 and NCI-H1975-OSR1 lines, AC0010 was more potent than both osimertinib and rociletinib. However, such phenomena can be seen in both osimertinib and AC0010-induced resistant cell lines, but not in the resistant cell line generated from relapsed mouse tumor tissues (Supplementary Table S4). Although the duration of tumor growth inhibition by AC0010 was demonstrated, the relationship between duration of EGFR T790M phosphorylation inhibition and tumor growth inhibition/resistance development was not analyzed in this study. A further investigation together with the resistance development and relevant mechanisms studies for exploring functional uniqueness of AC0010 is ongoing and will be reported separately.

AC0010 and its metabolites show no off-target effects and no skin lesion in animal models

As indicated previously, AC0010 showed adequate selectivity in kinase panel screening assay and additional 55 targets, including receptors, ion channels, and transporters (Supplementary Fig. S2; Supplementary Table S2). To further evaluate the safety liability of AC0010 metabolites, we elucidated the structures of six metabolites found in rats, monkey, or patients and proposed the AC0010 metabolic pathways (Fig. 4A). On the basis of preliminary human data, none of these metabolites are observed at exposures greater than 10 % of total drug-related exposure. We further evaluated three of these phase I and phase II metabolites that are observed with the highest exposures in patients, which include M7 (double bond reduction), MII-2 (cysteine conjugate), and MII-6 (N-acetylation of M4). All three major metabolites exhibited no toxicity against a panel of cell lines (Supplementary Table S5) and showed no activities against either wild-type or mutant EGFR in both cell proliferation and EGFR phosphorylation assays (Fig. 4B). No potent inhibitory activities against insulin-like growth factor 1 receptor (IGF-1R) were detected for M7, MII-2, and MII-6 (Supplementary Table S6). Accordingly, no hyperglycemia was seen in patients receiving AC0010 treatment (Table 1). The bioactive metabolite (M502) of rociletinib showed a strong inhibitory activity against IGF-1R (Supplementary Table S6) and exhibited unexpectedly high exposures in patients (22), which results in hyperglycemia in patients. The major metabolite (AZ5104) of osimertinib showed much more potent activity to both wild-type EGFR and mutant EGFR than its parent compound osimertinib (21). The lack of activities of the major metabolites of AC0010 against the wild-type EGFR and IGF-1R strongly indicates that AC0010 might have a unique safety profile in patients in comparison with osimertinib and rociletinib.

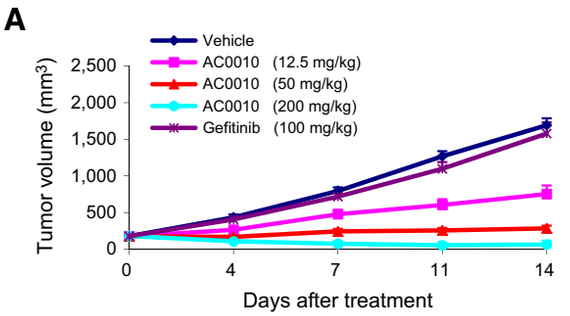

Days posttreatment	D4	D7	D11	D14
AC0010 12.5 mg/kg (%)	41	43	56	60
AC0010 50 mg/kg (%)	64	71	81	85
AC0010 200 mg/kg (%)	79	93	97	98
Gefitinib 100 mg/kg (%)	8	12	16	12

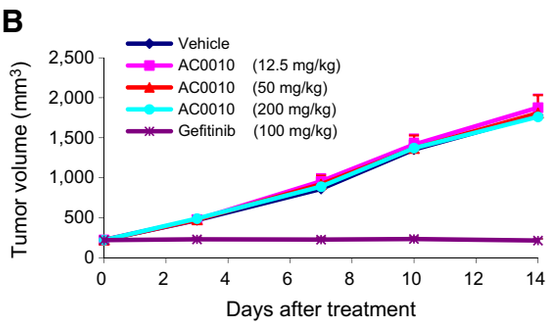

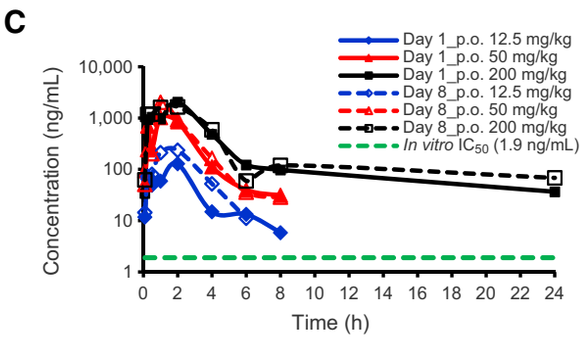

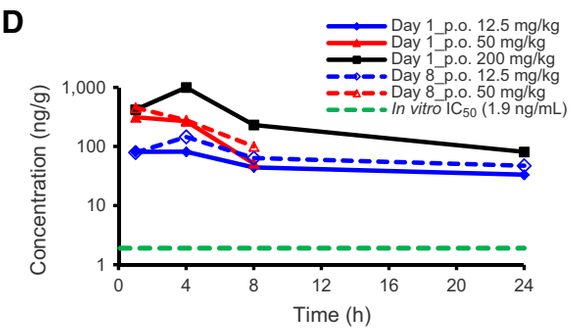

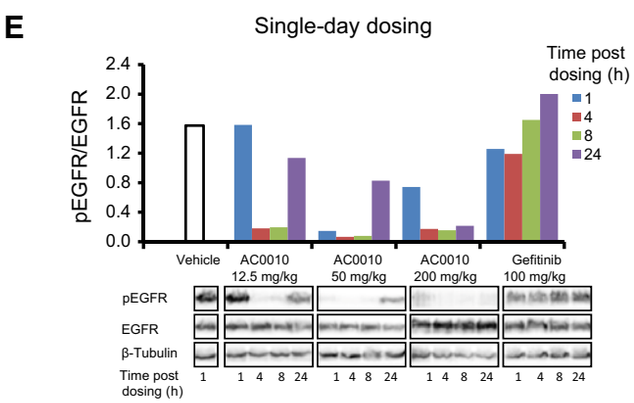

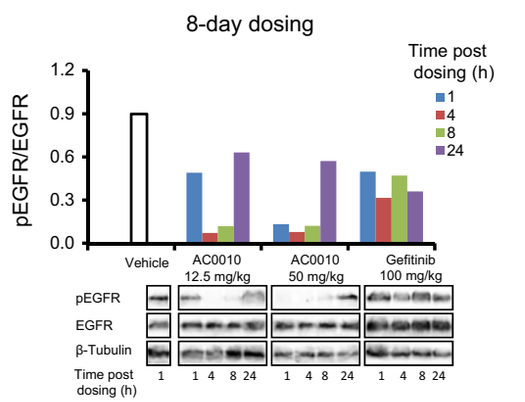

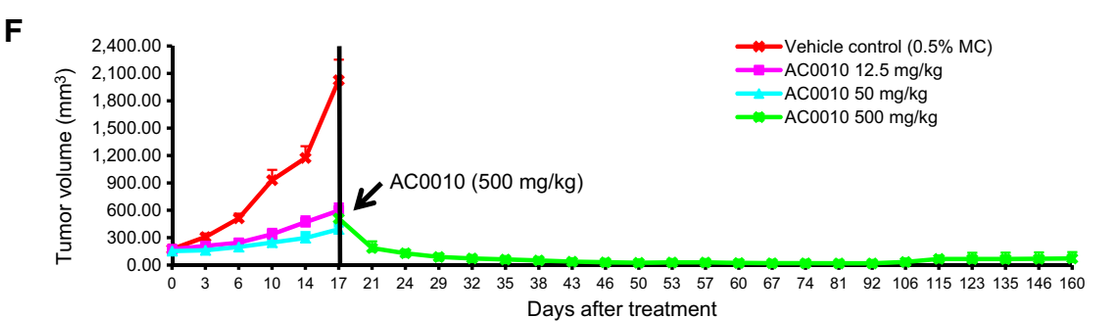

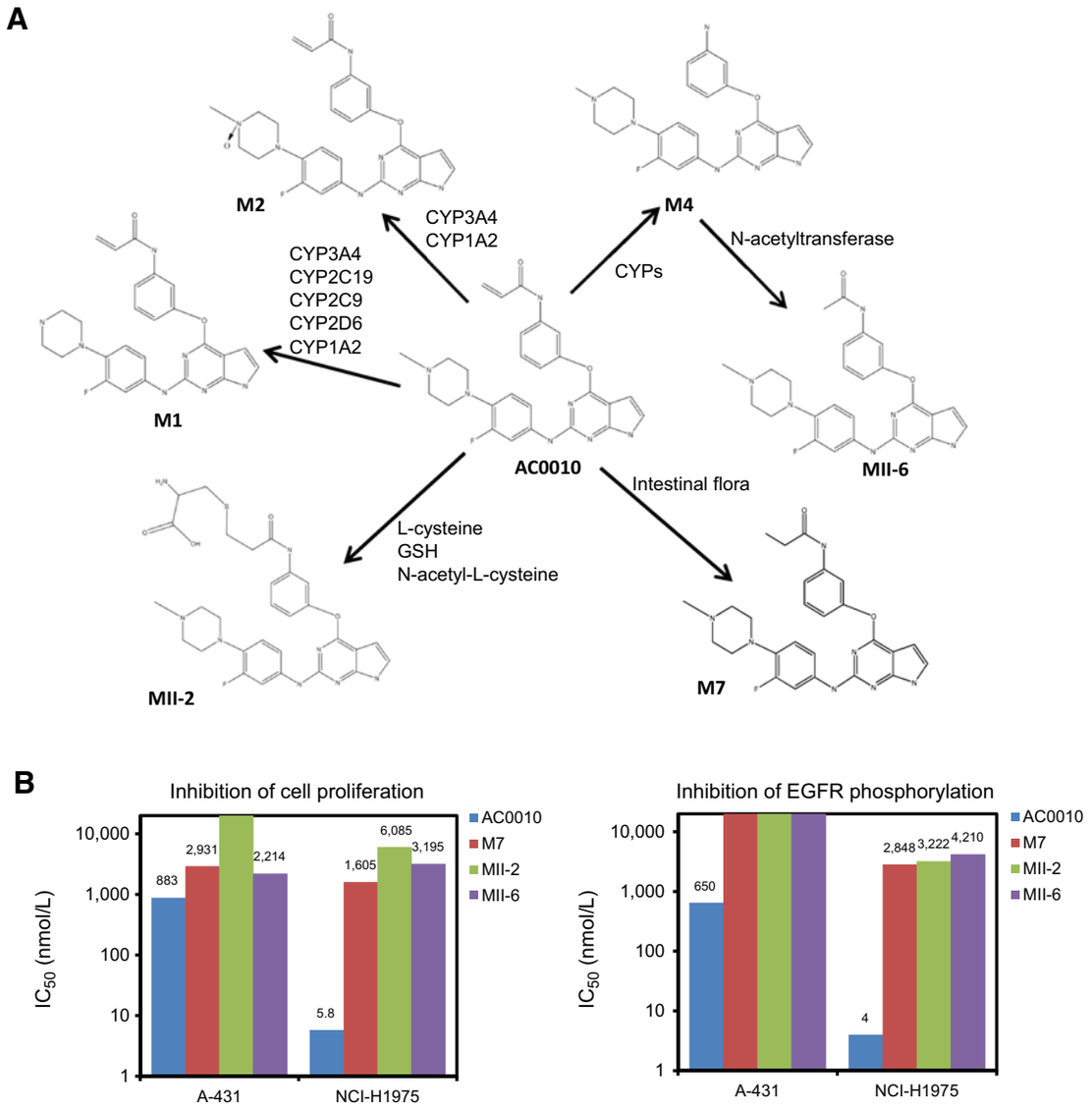

Figure 4.

Proposed AC0010 metabolic pathways and activities of its major metabolites. **A,** proposed AC0010 metabolic pathways showing the formation of metabolites through N-demethylation (M1), N-oxidation (M2), and N-dealkylation (M4) followed by acetylation (MII-6), reduction (M7), and cysteine conjugation (MII-2). **B,** inhibitory activities of AC0010 and its metabolites on cell proliferation by WST assay and EGFR phosphorylation in NCI-H1975 and A431 cells by ELSA. The IC_{50} values are indicated.

Figure 3.

In vivo antitumor efficacy and pharmacokinetics/pharmacodynamics in xenograft models. **A,** inhibition of NCI-H1975 tumor growth by AC0010 and gefitinib. Tumor growth curves are plotted as mean ± SEM ($n = 8$), and the inhibition rates in each treated group are indicated. **B,** inhibition of A431 tumor growth by AC0010 and gefitinib. Tumor growth curves are plotted as mean ± SEM ($n = 8$). **C,** AC0010 concentrations in plasma from AC0010-treated mice on days 1 and 8. The doses are indicated. p.o., oral administration. **D,** AC0010 concentrations in tumor tissues from AC0010-treated mice on days 1 and 8. Each dosing group is indicated. **E,** inhibition of EGFR phosphorylation in tumor tissues by AC0010 and gefitinib. pEGFR/EGFR values were derived from the densities of blotting bands of phosphorylated EGFR and total EGFR in NCI-H1975 tumor tissues from AC0010-treated mice after a single dose (top left) or after the last treatment of 8-day consecutive dosing (top right). The values (ratios) are indicated in the *y*-axis, and the lower number of pEGFR/EGFR indicates stronger inhibition. **F,** duration of antitumor efficacy and safety of AC0010 in subcutaneous xenograft NCI-H1975 mouse model. NCI-H1975 tumor-bearing mice were orally treated with vehicle control [0.5% methylcellulose (MC)] and AC0010 at dose levels of 12.5 and 50 mg/kg for 17 days when the tumor volume in vehicle control group reached approximately 2,000 mm^3. After 17-day dosing, the animals in vehicle control group were sacrificed, whereas animals in AC0010 groups were treated with increased dose at 500 mg/kg once per day for another 143 days. The tumor volume changes following total 160-day treatment of AC0010 are plotted as mean ± SEM.

Table 1. AEs of evaluable-for-safety population in AC0010 dose–escalation stage ($N = 25$)

	AC0010 dose–escalation stage ($N = 25$)											
	50 mg ($n = 4$)		100 mg ($n = 5$)		200 mg ($n = 7$)		350 mg ($n = 3$)		550 mg ($n = 6$)		Total ($N = 25$)	
CTCAE grades	All	≥3	All	≥3	All	≥3	All	≥3	All	≥3	All	≥3
	Number of patients (%)											
Skin and subcutaneous tissue disorders												
Rash	0 (0)	0 (0)	0 (0)	0 (0)	2 (29)	0 (0)	1 (33)	0 (0)	2 (33)	1 (17)	5 (20)	1 (4)
Pruritus	0 (0)	0 (0)	0 (0)	0 (0)	1 (14)	0 (0)	1 (33)	0 (0)	2 (33)	0 (0)	4 (16)	0 (0)
Hyperpigmentation	1 (25)	0 (0)	0 (0)	0 (0)	0 (0)	0 (0)	0 (0)	0 (0)	1 (17)	0 (0)	2 (8)	0 (0)
Hand-foot syndrome	0 (0)	0 (0)	0 (0)	0 (0)	1 (14)	0 (0)	0 (0)	0 (0)	0 (0)	0 (0)	1 (4)	0 (0)
Gastrointestinal disorders												
Diarrhea	1 (25)	0 (0)	0 (0)	0 (0)	1 (14)	0 (0)	3 (100)	0 (0)	6 (100)	0 (0)	11 (44)	0 (0)
Nausea	0 (0)	0 (0)	0 (0)	0 (0)	0 (0)	0 (0)	2 (67)	0 (0)	2 (33)	0 (0)	4 (16)	0 (0)
Laboratory tests												
Aminotransferase increased	1 (25)	0 (0)	0 (0)	0 (0)	0 (0)	0 (0)	0 (0)	0 (0)	0 (0)	0 (0)	1 (4)	0 (0)
WBC count decreased	1 (25)	0 (0)	0 (0)	0 (0)	1 (14)	0 (0)	0 (0)	0 (0)	1 (17)	0 (0)	3 (12)	0 (0)
Respiratory, thoracic, and mediastinal disorders												
Cough	1 (25)	0 (0)	2 (40)	0 (0)	2 (29)	0 (0)	0 (0)	0 (0)	2 (33)	0 (0)	7 (28)	0 (0)
Hemoptysis	1 (25)	0 (0)	2 (40)	0 (0)	0 (0)	0 (0)	0 (0)	0 (0)	0 (0)	0 (0)	3 (12)	0 (0)
Dyspnea	0 (0)	0 (0)	0 (0)	0 (0)	2 (29)	0 (0)	0 (0)	0 (0)	1 (17)	0 (0)	3 (12)	0 (0)
Nervous system disorders												
Paresthesia	0 (0)	0 (0)	1 (20)	0 (0)	0 (0)	0 (0)	0 (0)	0 (0)	0 (0)	0 (0)	1 (4)	0 (0)
Dizziness	1 (25)	0 (0)	0 (0)	0 (0)	0 (0)	0 (0)	0 (0)	0 (0)	0 (0)	0 (0)	1 (4)	0 (0)
AEs of interest												
Hyperglycemia	0 (0)	0 (0)	0 (0)	0 (0)	0 (0)	0 (0)	0 (0)	0 (0)	0 (0)	0 (0)	0 (0)	0 (0)
QT prolongation	0 (0)	0 (0)	0 (0)	0 (0)	2 (29)	0 (0)	0 (0)	0 (0)	0 (0)	0 (0)	2 (8)	0 (0)
Pneumonia	0 (0)	0 (0)	0 (0)	0 (0)	0 (0)	0 (0)	0 (0)	0 (0)	0 (0)	0 (0)	0 (0)	0 (0)

Abbreviation: WBC, white blood cell.

To further assess the potential skin toxicity of AC0010, a rat model was used. Rats were administrated daily with AC0010 at 300 mg/kg for 4 weeks, and in control groups, gefitinib at 50 mg/kg or vehicle control (0.5% methylcellulose) was administrated. Results showed that the skin lesions were observed in gefitinib-treated group, whereas, no apparent skin damage was found in AC0010-treated group (Supplementary Fig. S4).

AC0010 is safe and overcomes T790M-induced resistance in NSCLC patients

In this study, 25 patients were enrolled in a dose–escalation study (Supplementary Table S7). Only 1 DLT was observed at the dose level of 550 mg/day, where a female patient had developed a CTCAE grade 3 rash, due to the allergy to AC0010 (Table 1) but not to the inhibition of wild-type EGFR. AEs of any grade and of grade 3 or higher are summarized in Table 1. The most common AEs considered to be drug related were diarrhea (44% of patients), rash (20% of patients), and pruritus (16%). Although diarrhea and rash increased in frequency in a dose-dependent manner, the majority of them were grade 1. There was no drug discontinuation in all treated patients. No pneumonitis, hyperglycemia, or grade 3 prolongation of the corrected QT interval event was observed in these 25 patients.

Two relapsed NSCLC patients with positive EGFR T790M mutation detected in the biopsy samples after first-generation EGFR TKI treatment were treated with AC0010 at dose levels of 100 and 550 mg, and radiographic responses were confirmed with both patients (Fig. 5A and B). The first patient was a 59-year-old female with stage IV disease. The patient received 6 cycles of pemetrexed plus cisplatin as first-line chemotherapy, followed by the treatments with 2 cycles of pemetrexed, EGFR TKI (gefitinib) for 27 months, 2 cycles of pemetrexed plus Avastin, 6 cycles of pemetrexed plus cisplatin, and 1 cycle of docetaxel plus capecitabine. The patient was enrolled to receive AC0010 treatment at 100 mg dose cohort. Tumor shrinkage of 20% was detected after the first cycle treatment (4 weeks) and 31% after three cycle treatments (12 weeks; Fig. 5A). The second NSCLC patient was a 48-year-old male with stage IV disease. The patient received 3 cycles of pemetrexed plus carboplatin regimen as first-line chemotherapy, followed by gefitinib treatment for 41 months until the tumor relapsed. The patient was enrolled to receive AC0010 treatment at 550 mg dose cohort. Tumor shrinkage of 33% was detected after the first cycle treatment and 36% after three cycle treatments (Fig. 5B). Figure 5C shows the plasma pharmacokinetic profiles of the two patients after dosing at 100 and 550 mg once per day for 28 days, respectively.

Discussion

In recent clinical studies, the third-generation EGFR inhibitors, such as osimertinib and rociletinib, are capable of inhibiting mutant EGFR with T790M and produce responses in more than 50% of patients who acquired the resistance against first-generation EGFR TKIs (18, 19). Structurally, osimertinib, rociletinib, and previously reported tool compound WZ4002 are pyrimidine-based EGFR TKIs (17, 20–21). The new EGFR TKI, AC0010, reported in this study is a pyrrolopyrimidine-based third-generation EGFR TKI, which is structurally distinct from the currently reported third-generation EGFR TKIs. Using the docking model, the pyrrolopyrimidine core of AC0010 showed more stable binding than the pyrimidine core in tool compound WZ4002 in a computer-added model, and such stable binding also correlated well with the increase in the inhibitory potency of the mutant EGFR with T790M and a good selectivity over wild-type EGFR (Fig. 2). In both cell-based

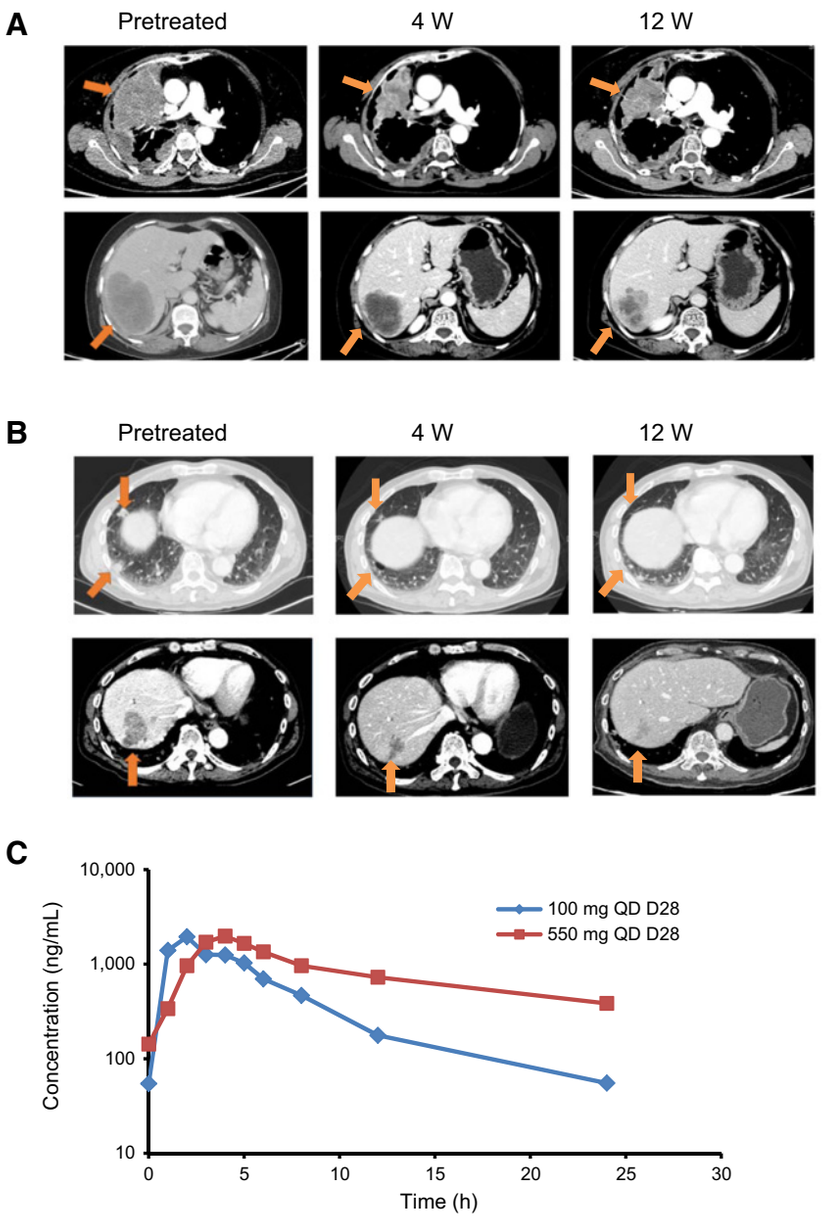

Figure 5.
Response of NSCLC patients with T790M-acquired mutations to AC0010 treatment and their AC0010 plasma concentrations. **A,** NCSLC patients received AC0010 treatment at a dose of 100 mg once per day for three cycles (28 days/cycle). The lesions indicated by arrows are shown in the CT images of lung (top) and liver (bottom). **B,** NCSLC patients received AC0010 treatment at a dose of 550 mg once per day for three cycles. The lesions indicated by arrows are shown in the CT images of lung (top) and liver (bottom). **C,** AC0010 from patients treated at doses of 100 and 550 mg per day. AUC_{0-24h} values were 10,800 and 19,500 ng·h/mL for patients receiving 100 mg per day (**A**) and for patients receiving 550 mg per day (**B**), respectively. QD, every day.

assays and animal models, AC0010 revealed the unique features of the third-generation EGFR TKI previously reported in other third-generation EGFR TKIs (17, 20–21), which include (i) irreversibly binding EGFR by forming a covalent bound with Cys 797 in the ATP-binding pocket (Supplementary Fig. S1); (ii) sparing wild-type EGFR; and (iii) overcoming T790M-induced resistance (Figs. 2 and 3). In *in vivo* duration study, 14 mice bearing the NCI-H1975 tumors were treated with AC0010 daily for 160 days, and tumors in 12 of 14 mice were inhibited during the 160-day treatment, suggesting the durable inhibition activity of AC0010. However, tumor relapses were detected in two mice at days 106 and 135, indicating acquisition of resistance against AC0010 may have developed in these two mice. Acquired drug resistance was also seen in the clinical studies of pyrimidine-based irreversible EGFR inhibitors, such as osimertinib and rociletinib (23–26). The resistance against the newly developed third-generation EGFR TKIs will significantly limit the long-term clinical success of third-generation EGFR TKIs. Results from nonclinical study models indicated that mechanisms by which the third-generation EGFR TKIs, including WZ4002, osimertinib, and rociletinib, induce resistance were similar and drugs are cross-resistant (27). Emerging clinical data also revealed that the C797S mutation is detected in approximately 40% of EGFR-mutant NSCLC patients with T790M who developed acquired resistance to osimertinib (23). Interestingly, some EGFR-resistant mutations induced by pyrimidine-based irreversible EGFR inhibitors, such as exon19 Del/C797S, are still sensitive to quinazoline-based EGFR inhibitors gefitinib and afatinib (27, 28). Therefore, irreversible EGFR inhibitors with different chemical core structure may reveal different resistant mechanisms. Using resistant cells derived from AC0010 long-term treated xenograft tumors and

drug-induced resistant clones from cell cultures, we found that AC0010 showed cross-resistance with other third-generation compounds, such as osimertinib and rociletinib. However, our preliminary data showed that the resistance level is different between AC0010 and osimertinib (Supplementary Table S4). Studies to further understand the underlying mechanisms of acquired resistance against third-generation EGFR TKIs with different chemical structures are warranted to help us design better clinical treatment strategies for patients to gain maximum benefits from EGFR-TKI–based target therapy.

The preclinical pharmacokinetics/pharmacodynamics study demonstrated that the tumor inhibition of AC0010 is well correlated with duration of inhibition of EGFR phosphorylation in NCI-H1975 tumors (Fig. 3). At the dose of 200 mg/kg, the double mutant EGFR phosphorylation can be completely inhibited for 24 hours, resulting in 98% tumor growth inhibition, which suggests that the persistent exposure of AC0010 is required to gain the best therapeutic advantage in NSCLC patients. On the basis of the efficacy data of three EGFR-mutant xenograft mouse models at 50 and 200 mg/kg, which resulted in stable and regressive xenograft tumors, respectively, the human efficacious dose projected based on body surface area conversion factor (12.3) can be predicated to be in the range of 244 and 976 mg per day for a 60-kg human. Notably, in the phase I clinical trial (NCT02274337), a patient was responsive to AC0010 at the dose of 100 mg once per day (Fig. 5A). Interestingly, for this responsive case, AC0010 blood exposure was high, reaching to AUC_{0-24h} value of 10,800 ng·h/mL, which is above blood drug exposure at the effective doses in the mouse model, and close to the drug exposure of the patient at the dose of 550 mg per day (ACU_{0-24h} value, 19,500 ng·h/mL), who was also responsive to AC0010 (Fig. 5B). Detailed clinical pharmacokinetics study will be reported in separate reports.

The selective inhibition of the mutant EGFR by third-generation EGFR inhibitors greatly improves the on-target AEs that resulted from the equal inhibition of both wild-type and mutant EGFR by first-generation EGFR TKIs and second-generation EGFR TKIs, such as afatinib (29–31). In the rat model, AC0010 showed no skin lesion after 28-day treatment at a dose as high as 300 mg/kg (Supplementary Fig. S4). In clinical study, although the patient number is still small, much less occurrence of rash (24%) was seen in the patients treated with AC0010 and most of them were grade 1. Both in animal safety studies (data not shown) and in clinical trials, no severe off-target effects induced by AC0010 parent drug and its metabolites were seen, which indeed is consistent with weak to no binding of 55 safety-related target screening (Supplementary Table S2) and results from the biological analysis on AC0010 metabolite profile (Fig. 4). Off-target–related AEs were reported in patients who received the treatment of rociletinib (19). The predominant AE of rociletinib is hyperglycemia, which occurred in 47% of tested patients and 22% of them are grade 3. Hyperglycemia is caused by a rociletinib metabolite that inhibits IGF-1R (Supplementary Table S6; refs. 19, 22). AC0010 parent compound and three major metabolites do not inhibit IGF-1R (Supplementary Table S6). As a consequence, no hyperglycemia was detected in rats and monkeys in the long-term animal safety studies (data not shown) and in patients enrolled in the phase I dose–escalation study (Table 1). Furthermore, the three major metabolites of AC0010 revealed no inhibitory activity against either wild-type EGFR or mutant EGFR in contrast to a metabolite of osimertinib (AZ5104). Indeed, in patients, osimertinib showed frequent wild-type EGFR inhibition-related AEs, such as skin damage (40%), which might also have been resulted from the very potent activities of AZ5104 (21). Minimal effects on IGF1-R, on the other hand, were reported for osimertinib (32). The different safety profile of AC0010 and its major metabolites strongly suggests that AC0010 is distinct from the other two third-generation EGFR inhibitors, osimertinib and rociletinib.

AC0010 is a new third-generation EGFR inhibitor and showed potent activity against EGFR T790M mutation. Because of its distinct structure and metabolite profile, AC0010 might demonstrate unique therapeutic property in future clinical trials and provide another option for patients who develop resistance against first-generation EGFR inhibitors or for combination therapy with other anticancer agents.

Disclosure of Potential Conflicts of Interest

X. Xu has ownership interest (including patents) in ACEA Biosciences. C. Fang has ownership interest in ACEA stock. No potential conflicts of interest were disclosed by the other authors.

Authors' Contributions

Conception and design: X. Xu, L. Mao, W. Xu, B. Xi, L. Zhao, X. Wang, P. Hu, L. Zhang

Development of methodology: L. Mao, W. Xu, W. Tang, X. Zhang, B. Xi, R. Xu, J. Liu, C. Fang, L. Zhao, X. Wang, P. Hu, L. Zhang

Acquisition of data (provided animals, acquired and managed patients, provided facilities, etc.): X. Xu, W. Xu, W. Tang, X. Zhang, B. Xi, R. Xu, X. Fang, C. Fang, L. Zhao, L. Zhang

Analysis and interpretation of data (e.g., statistical analysis, biostatistics, computational analysis): X. Xu, W. Xu, W. Tang, B. Xi, R. Xu, X. Fang, C. Fang, L. Zhao, X. Wang, P. Hu, H. Zhao, L. Zhang

Writing, review, and/or revision of the manuscript: X. Xu, L. Mao, W. Xu, W. Tang, X. Zhang, B. Xi, R. Xu, C. Fang, L. Zhao, X. Wang, H. Zhao, L. Zhang

Administrative, technical, or material support (i.e., reporting or organizing data, constructing databases): X. Xu, W. Xu, W. Tang, X. Zhang, R. Xu, X. Fang, J. Liu, C. Fang, L. Zhao, X. Wang, L. Zhang

Study supervision: X. Xu, L. Mao, W. Xu, W. Tang, X. Zhang, R. Xu, X. Fang, J. Liu, C. Fang, X. Wang, J. Jiang, L. Zhang

Other (lead of AC0010 medicinal chemistry project, designed and performed compound discovery and synthesis, and helped in the preparation of the manuscript): L. Mao

Acknowledgments

We acknowledge Professor Jin Ma of National Shanghai Center for New Drug Safety Evaluation and Research for the leadership of the preclinical toxicology and drug safety, Dr. Donald Hou and Laibao Wang of ChemPartner for drug substance manufacturing, and Dr. Na Zhao and Anand Kulkarni of WuXi AppTec for drug product manufacture. We also acknowledge Dr. Yama Abassi for the input in manuscript preparation.

Grant Support

The work was supported by China Twelfth Five-Year Plan Key Project (grant 2013ZX09401003; to X. Xu) and Hangzhou Municipal Key Project (grant 2014-1249; to X. Xu).

The costs of publication of this article were defrayed in part by the payment of page charges. This article must therefore be hereby marked *advertisement* in accordance with 18 U.S.C. Section 1734 solely to indicate this fact.

Received May 6, 2016; revised July 28, 2016; accepted August 9, 2016; published OnlineFirst August 29, 2016.

References

1. Herbst RS, Heymach JV, Lippman SM. Lung cancer. N Engl J Med 2008; 359:1367–80.
2. Sher T, Dy GK, Adjei AA. Small cell lung cancer. Mayo Clin Proc 2008; 83:355–67.
3. Paez JG, Janne PA, Lee JC, Tracy S, Greulich H, Gabriel S, et al. EGFR mutations in lung cancer: correlation with clinical response to gefitinib therapy. Science 2004;304:1497–500.
4. Soda M, Choi YL, Enomoto M, Takada S, Yamashita Y, Ishikawa S, et al. Identification of the transforming EML4–ALK fusion gene in non-small-cell lung cancer. Nature 2007;448:561–6.
5. The Cancer Genome Atlas Research Network (TCGA). Comprehensive genomic characterization of squamous cell lung cancers. Nature 2012; 489:519–25.
6. Sequist LV, Martins RG, Spigel D, Grunberg SM, Spira A, Janne PA, et al. First-line gefitinib in patients with advanced non-small-cell lung cancer harboring somatic EGFR mutations. J Clin Oncol 2008;26:2442–9.
7. Mok TS, Wu YL, Thongprasert S, Yang CH, Chu DT, Saijo N, et al. Gefitinib or carboplatin-paclitaxel in pulmonary adenocarcinoma. N Engl J Med 2009;361:947–57.
8. Fukuoka M, Wu YL, Thongprasert S, Sunpaweravong P, Leong SS, Sriuranpong V, et al. Biomarker analyses and final overall survival results from a phase III, randomized, open-label, first-line study of gefitinib versus carboplatin/paclitaxel in clinically selected patients with advanced non–small-cell lung cancer in Asia (IPASS). J Clin Oncol 2011;29:2866–74.
9. Lynch TJ, Bell DW, Sordella R, Gurubhagavatula S, Okimoto RA, Brannigan BW, et al. Activating mutations in the epidermal growth factor receptor underlying responsiveness of non-small-cell lung cancer to gefitinib. N Engl J Med 2004;350:2129–39.
10. Jackman D, Pao W, Riely GJ, Engelman JA, Kris MG, Janne PA, et al. Clinical definition of acquired resistance to epidermal growth factor receptor tyrosine kinase inhibitors in non-small-cell lung cancer. J Clin Oncol 2010;28:357–60.
11. Yu HA, Arcila ME, Rekhtman N, Sima CS, Zakowski MF, Pao W, et al. Analysis of tumor specimens at the time of acquired resistance to EGFR-TKI therapy in 155 patients with EGFR-mutant lung cancers. Clin Cancer Res 2013;19:2240–7.
12. Pao W, Miller VA, Politi KA, Riely GJ, Somwar R, Zakowski MF, et al. Acquired resistance of lung adenocarcinomas to gefitinib or erlotinib is associated with a second mutation in the EGFR kinase domain. PLoS Med 2005;2:e73.
13. Yun CH, Mengwasser KE, Toms AV, Woo MS, Greulich H, Wong KK, et al. The T790M mutation in EGFR kinase causes drug resistance by increasing the affinity for ATP. Proc Natl Acad Sci U S A 2008;105:2070–5.
14. Gazdar A. Activating and resistance mutations of EGFR in non-small-cell lung cancer: role in clinical response to EGFR tyrosine kinase inhibitors. Oncogene 2009;28(Suppl 1):S24–S31.
15. Niederst MJ, Engelman JA. Bypass mechanisms of resistance to receptor tyrosine kinase inhibition in lung cancer. Sci Signal 2013;6:re6.
16. Kobayashi S, Boggon TJ, Dayaram T, Jänne PA, Kocher O, Meyerson M, et al. EGFR mutation and resistance of non–small-cell lung cancer to gefitinib. N Engl J Med 2005;352:786–92.
17. Zhou W, Ercan D, Chen L, Yun CH, Li D, Capelletti M, et al. Novel mutant-selective EGFR kinase inhibitors against EGFR T790M. Nature 2009;462: 1070–4.
18. Jänne PA, Yang JC, Kim DW, Planchard D, Ohe Y, Ramalingam SS, et al. AZD9291 in EGFR inhibitor–resistant non–small-cell lung cancer. N Engl J Med 2015;371:1689–99.
19. Sequist LV, Soria JC, Goldman JW, Wakelee HA, Gadgeel SM, Varga A, et al. Rociletinib in EGFR-mutated non–small-cell lung cancer. N Engl J Med 2015;372:1700–9.
20. Walter AO, Sjin RT, Haringsma HJ, Ohashi K, Sun J, Lee K, et al. Discovery of a mutant-selective covalent inhibitor of EGFR that overcomes T790M-mediated resistance in NSCLC. Cancer Discov 2013;3:1404–15.
21. Cross DA, Ashton SE, Ghiorghiu S, Eberlein C, Nebhan CA, Spitzler PJ, et al. AZD9291, an irreversible EGFR TKI, overcomes T790M-mediated resistance to EGFR inhibitors in lung cancer. Cancer Discov 2014;4: 1046–61.
22. Simmons AD, Tsai SJ, Haringsma HJ, Allen A, Harding TC. Insulin-like growth factor 1 (IGF1R)/insulin receptor (INSR) inhibitory activity of rociletinib (CO-1686) and its metabolites in nonclinical models. In: Proceedings of the 106th Annual Meeting of the American Association for Cancer Research; 2015 Apr 18–22; Philadelphia, PA. Philadelphia (PA): AACR; 2015. Abstract nr 793.
23. Thress KS, Paweletz CP, Felip E, Cho BC, Stetson D, Dougherty B, et al. Acquired EGFR C797S mediates resistance to AZD9291 in advanced non-small cell lung cancer harboring EGFR T790M. Nat Med 2015;21:560–2.
24. Yu HA, Tian SK, Drilon AE, Borsu L, Riely GJ, Arcila ME, et al. Acquired resistance of EGFR-mutant lung cancer to a T790M-specific EGFR inhibitor emergence of a third mutation (C797S) in the EGFR tyrosine kinase domain. JAMA Oncol 2015;1:982–4.
25. Haringsma HJ, Allen A, Harding TC, Simmons AD. *In vivo* acquired resistance to the mutant EGFR inhibitor rociletinib (CO-1686) is associated with activation of the c-MET pathway. In: Proceedings of the 106th Annual Meeting of the American Association for Cancer Research; 2015 Apr 18–22; Philadelphia, PA. Philadelphia (PA): AACR; 2015. Abstract nr 3595.
26. Piotrowska Z, Niederst MJ, Karlovich CA, Wakelee HA, Neal JW, Mino-Kenudson M, et al. Heterogeneity underlies the emergence of EGFR T790 wild-type clones following treatment of T790M-positive cancers with a third generation EGFR inhibitor. Cancer Discov 2015;5:713–22.
27. Ercan D, Choi HG, Yun CH, Capelletti M, Xie T, Eck MJ, et al. EGFR mutations and resistance to irreversible pyrimidine-based EGFR inhibitors. Clin Cancer Res 2015;21:3913–23.
28. Niederst MJ, Hu H, Mulvey HE, Lockerman EL, Garcia AR, Piotrowska Z, et al. The allelic context of the C797S mutation acquired upon treatment with third-generation EGFR inhibitors impacts sensitivity to subsequent treatment strategies. Clin Cancer Res 2015;21:3924–33.
29. Mitsudomi T, Morita S, Yatabe Y, Negoro S, Okamoto I, Tsurutani J, et al. Gefitinib versus cisplatin plus docetaxel in patients with non-small-cell lung cancer harbouring mutations of the epidermal growth factor receptor (WJTOG3405): an open label, randomised phase 3 trial. Lancet Oncol 2010;11:121–8.
30. Miller VA, Hirsh V, Cadranel J, Chen YM, Park K, Kim SW, et al. Afatinib versus placebo for patients with advanced, metastatic non–small-cell lung cancer after failure of erlotinib, gefitinib, or both, and one or two lines of chemotherapy (LUX-Lung 1): a phase 2b/3 randomised trial. Lancet Oncol 2012;13:528–38.
31. Sequist LV. Second-generation epidermal growth factor receptor tyrosine kinase inhibitors in non-small cell lung cancer. Oncologist 2007; 12:325–30.
32. Finlay MR, Anderton M, Ashton S, Ballard P, Bethel PA, Box MR, et al. Discovery of a potent and selective EGFR inhibitor (AZD9291) of both sensitizing and T790M resistance mutations that spares the wild type form of the receptor. J Med Chem 2014;57:8249–67.